Optimal and Adaptive Mismatch Filtering for Stretch Processing

Lumumba Harnett[1], Dana Hemmingsen[1], Patrick M. McCormick[1], Shannon D. Blunt[1], Christopher Allen[1]
Anthony Martone[2], Kelly Sherbondy[2], David Wikner[2]
[1]Radar Systems Lab (RSL), University of Kansas, Lawrence, KS
[2]Army Research Laboratory (ARL), Washington, DC

***Abstract*—Traditional stretch processing performs match filtering using a Fourier transform, which is essentially the matched filter bank for an LFM waveform mixed with an LFM reference. Here we consider how optimal least-squares based mismatched filtering could be used in place of the Fourier transform. This notion is then taken a step further with the formulation of an adaptive transformation. These new stretch processing filter structures are demonstrated in simulation and experimentally using open-air measurements, with the enhancements they enable applicable to a wide variety of legacy systems.**

Keywords—Stretch processing, waveform diversity, mismatch filtering, adaptive filtering

I. Introduction

Stretch processing was proposed by Caputi in 1971 [1] as a means to transform the time scale of signals. Since then it has become a mainstay of wideband radar systems [2] and is one of the main reasons that the linear FM (LFM) waveform has been so widely used for more than 50 years [3], despite its high range sidelobes. Specifically, stretch processing permits high range resolution to be achieved without requiring receive sampling at the high rate that would otherwise be necessary for wideband waveforms.

Given the echoes from a wideband LFM waveform, stretch processing operates by receive-mixing these echoes with a reference LFM having the same chirp rate as the transmitted waveform. This action serves to convert the individual reflected echoes of the transmitted LFM waveform into a weighted sum of sinusoids, where the frequency of each sinusoid corresponds to range delay and the associated weighting is the complex scattering at that delay. This mixing stage also achieves some degree of frequency down-conversion depending on the amount of frequency offset between the waveform and reference. Subsequent filtering, additional down-conversion, and in-phase/quadrature-phase (IQ) sampling then realizes a digitized complex signal for which the Fourier transform serves as a matched filter bank.

In a companion paper [4] it has been experimentally demonstrated that it is possible to employ the stretch processing RF receive chain for pulse compression of chirp-like nonlinear FM (NLFM) waveforms (e.g. [5-13]) by replacing the standard Fourier transform after digitization with a compensation transform. The work in [4] establishes the feasibility of using a wider variety of wideband waveforms for stretched processing, potentially enabling enhanced performance.

Here, we alternatively take the approach that the LFM waveform is unchanged but explore how optimal and adaptive mismatched filters could be employed such as in [14]. Mismatched filters have the advantage of minimizing peak and integrated sidelobes as a trade-off for some degree of mainlobe mismatch loss. Of course, it stands to reason that these alternative filters could likewise be paired with NLFM waveforms, but such is outside the scope of this paper.

Like [14], we examine the practical use of least-squares mismatched filters [15] and reiterative minimum mean-square error (RMMSE) adaptive filtering [16,17], albeit now within this stretch processing context. The important distinction to be made is that, where standard pulse compression involves a convolution process [14], the initial stretch processing stage in which the receive echoes are mixed with a reference LFM violates linear time invariance (LTI), such that the subsequent filtering process is not through convolution. That said, by alternatively viewing the final fast Fourier transform (FFT) stage as the application of a discrete Fourier transform (DFT) matched filter bank, it is possible to pose a framework for the development of optimal and adaptive mismatched filter banks.

II. Stretch Processing Signal Model

A pulsed LFM waveform, defined over $0 \le t \le T$ for pulsewidth T, can be expressed as

$$s(t) = \cos[2\pi f(t)\, t], \tag{1}$$

where the instantaneous frequency as a function of time is

$$f(t) = (f_{\text{start}} - f_{\text{end}})\frac{t}{T} \tag{2}$$

for f_{start} and f_{end} the start and end frequencies, respectively. Letting $x(t)$ represent the illuminated scattering as a function of range and ignoring nonlinear effects, the reflected signal can be written as

$$\tilde{y}(t) = s(t) * x(t) + u(t), \tag{3}$$

for $u(t)$ additive noise and $*$ the convolution operation.

As illustrated in Fig. 1, the subsequent RF mixing, bandpass filtering (BPF), and IQ demodulation processes collectively produce the complex, baseband signal

$$y(t) = y_{\text{I}}(t) + jy_{\text{Q}}(t) = \Phi_{\text{LPF}}\left\{y_{\text{IF}}(t) \times \exp\left(-j2\pi f_{\text{IF}} t\right)\right\} \tag{4}$$

that is then sampled by the analog-to-digital converter (ADC). Here, $y_{\text{I}}(t)$ and $y_{\text{Q}}(t)$ are the in-phase and quadrature-phase signal components, $\Phi_{\text{LPF}}\{\bullet\}$ is a lowpass filtering (LPF) operation, $y_{\text{IF}}(t)$ is the received signal after LFM reference

This work was supported in part by the Army Research Office under Contract # W911NF-15-2-0063, by the Army Research Laboratory under Contract # W911NF-16-2-0222, and by the NSF Graduate Research Fellowship Program under Grant No. DGE-1451148.

mixing with $s_{\text{ref}}(t)$ down to the intermediate frequency f_{IF}, and $\omega_{\text{IF}} = 2\pi f_{\text{IF}}$. Denote the sampled version of (4) as the length L vector $\mathbf{y}$ [4].

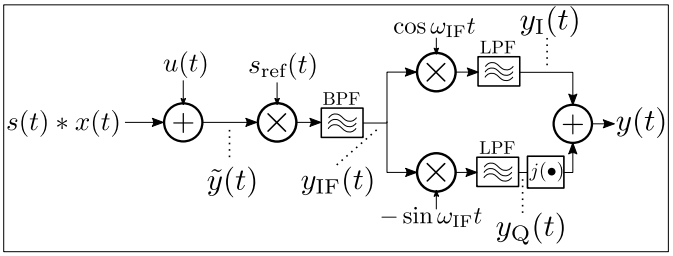

Fig. 1. Signal model of stretch processing receive chain

An LFM waveform reflected by a single hypothetical scatterer at range R, captured by the receive antenna, and passed through this RF receive chain would possess the structure

$$p(t,R) = \Phi_{\text{LPF}}\left\{\Phi_{\text{BPF}}\left\{s_{\text{ref}}(t) \times s\left(t - \frac{2R}{c}\right)\right\} \times \exp\left(-j2\pi f_{\text{IF}} t\right)\right\}, \quad (5)$$

which is a complex sinusoid scaled by the amplitude and phase of the particular scatterer, for $\Phi_{\text{BPF}}\{\bullet\}$ a bandpass filter operation and c the speed of light. The particular frequency of this sinusoid depends on the value of range R between the near and far range bounds R_{near} and R_{far}, respectively. Thus for the range swath $R \in [R_{\text{near}}, R_{\text{far}}]$ demarcated into N range samples, (5) can be discretized into a set of length L vectors $\mathbf{p}(n)$ for $n = 0, 1, \ldots, N-1$. Normalizing as

$$\mathbf{w}(n) = \frac{1}{\|\mathbf{p}(n)\|_2}\mathbf{p}(n) \quad (6)$$

therefore realizes the $L \times N$ matrix

$$\mathbf{W} = \left[\mathbf{w}(0) \quad \mathbf{w}(1) \quad \cdots \quad \mathbf{w}(N-1)\right], \quad (7)$$

the columns of which represent the structure of the expected signals discretely modelled as

$$\mathbf{y} = \mathbf{W}\mathbf{x} + \mathbf{u}, \quad (8)$$

for $\mathbf{x}$ the (over-sampled) length N vector of complex scattering over the range interval $[R_{\text{near}}, R_{\text{far}}]$ and the length L vector $\mathbf{u}$ the additive noise at the output of the ADC. To facilitate the fidelity required for the subsequent optimal and adaptive mismatched filter formulations, we have defined N to include over-sampling by a factor of K relative to the nominal range resolution associated with the bandwidth of the LFM waveform. Based on the model in (8), the operation

$$\hat{\mathbf{x}}_{\text{MF}} = \mathbf{W}^H\mathbf{y} \quad (9)$$

clearly yields the length N matched filter estimate that is simply an over-sampled version of the response that would be obtained by applying the FFT, with $(\bullet)^H$ the complex-conjugate transpose (or Hermitian) operation.

III. Stretch Processing Optimal Mismatch Filtering

The least-squares (LS) optimal mismatch filter was proposed in [15] for phase-coded waveforms. More recently it has been extended for application to arbitrary FM waveforms [14,18] where it is required to "over-sample" relative to the waveform 3-dB bandwidth to minimize the model mismatch effects that would otherwise limit sidelobe suppression and induce range straddling effects. In so doing, however, additional care must be taken to avoid imposing a range super-resolution condition [19] that is accompanied by increased sidelobes as a trade-off. This effect can be remedied by "spoiling" the mainlobe back to the nominal resolution of the matched filter [14]. The resulting mismatched filter provides significant sidelobe suppression with very small mismatch loss (fraction of a dB) without degrading resolution. Such a result is in contrast to traditional amplitude tapering prior to the FFT in stretch processing that reduces sidelobes at the cost of both resolution and possibly significant mismatch loss [20,21].

Since $\mathbf{W}$ and $\mathbf{x}$ were already specified in (7) and (8) as being over-sampled by K relative to the nominal resolution of the waveform, now define $\mathbf{D}$ as the $N \times N$ matrix

$$\mathbf{D} = \left(\mathbf{W}^H\mathbf{W}\right) \odot \mathbf{E}, \quad (10)$$

where $\mathbf{E}$ is an $N \times N$ banded Toeplitz matrix with ones on the main diagonal and on the $K-1$ diagonals above and below the main diagonal, and zeroes otherwise. Due to the over-sampling, the resulting $2K-1$ non-zero valued diagonals in $\mathbf{D}$ represent the complete mainlobe response to avoid super-resolution.

Using (10), the $L \times N$ mismatched filter bank is obtained by solving the least-squares cost function

$$J_{\text{LS}} = \left\|\mathbf{W}_{\text{MMF}}^H\mathbf{W} - \mathbf{D}\right\|_F^2 \quad (11)$$

for $\|\bullet\|_F$ the Frobenius norm. We can rewrite the cost function of (11) as

$$\begin{aligned}\left\|\mathbf{W}_{\text{MMF}}^H\mathbf{W} - \mathbf{D}\right\|_F^2 &= Tr\left\{\mathbf{W}_{\text{MMF}}^H\mathbf{W}\mathbf{W}^H\mathbf{W}_{\text{MMF}}\right\} \\ &\quad - Tr\left\{\mathbf{W}_{\text{MMF}}^H\mathbf{W}\mathbf{D}^H\right\} \\ &\quad - Tr\left\{\mathbf{D}\mathbf{W}_{\text{MMF}}\mathbf{W}^H\right\} + Tr\left\{\mathbf{D}\mathbf{D}^H\right\}\end{aligned}, \quad (12)$$

the gradient of which is

$$\nabla_{\mathbf{W}_{\text{MMF}}^*} J_{\text{LS}} = \mathbf{W}\mathbf{W}^H\mathbf{W}_{\text{MMF}} - \mathbf{W}\mathbf{D}^H. \quad (13)$$

Setting (13) equal to $\mathbf{0}_{L\times N}$ and then solving yields the mismatch filter bank

$$\mathbf{W}_{\text{MMF}} = \left(\mathbf{W}\mathbf{W}^H\right)^{-1}\mathbf{W}\mathbf{D}^H, \quad (14)$$

which can be diagonally loaded to avoid possible ill-conditioning effects as

$$\mathbf{W}_{\text{MMF}} = \left(\mathbf{W}\mathbf{W}^H + \delta\mathbf{I}_{L\times L}\right)^{-1}\mathbf{W}\mathbf{D}^H, \quad (15)$$

for δ a positive scalar and $\mathbf{I}_{L\times L}$ an $L \times L$ identity matrix. Application of this filter bank to the received data vector $\mathbf{y}$ results in the mismatch filter range profile estimate

$$\hat{\mathbf{x}}_{\text{MMF}} = \mathbf{W}_{\text{MMF}}^H\mathbf{y} = \mathbf{D}\mathbf{W}^H\left(\mathbf{W}\mathbf{W}^H + \delta\mathbf{I}_{L\times L}\right)^{-1}\mathbf{y} \quad (16)$$

for which range sidelobes are significantly suppressed while *a*) the range resolution of standard stretch processing is preserved and *b*) mismatch loss is quite small.

IV. Stretch Processing Adaptive Mismatch Filtering

An adaptive filter bank can likewise be obtained for the over-sampled signal model in (8) by using the reiterative super-resolution (RISR) algorithm [17], which can be derived from the mean-square error (MSE) cost function

$$J = E\left\{\left\|\mathbf{x} - \mathbf{W}_{\text{RISR}}^{H}\mathbf{y}\right\|_2^2\right\}, \tag{17}$$

for $E\{\bullet\}$ expectation. This cost function is minimized by

$$\mathbf{W}_{\text{RISR}} = \left(E\{\mathbf{y}\mathbf{y}^{H}\}\right)^{-1} E\{\mathbf{y}\mathbf{x}^{H}\}. \tag{18}$$

Substituting, (8) into (18) and assuming the scatterers are statistically uncorrelated, the adaptive filter bank becomes

$$\mathbf{W}_{\text{RISR}} = \left(\mathbf{W}\mathbf{P}\mathbf{W}^{H} + \mathbf{R}\right)^{-1}\mathbf{W}\mathbf{P}, \tag{19}$$

where

$$\mathbf{R} = E\{\mathbf{u}\mathbf{u}^{H}\} = \sigma_u^2\,\mathbf{I}_{L\times L} \tag{20}$$

and

$$\mathbf{P} = E\{\mathbf{x}\mathbf{x}^{H}\}, \tag{21}$$

for σ_u^2 the noise power.

Per [17], since $\mathbf{P}$ is not known *a priori* it is estimated iteratively using

$$\hat{\mathbf{P}}_i = \left(\hat{\mathbf{x}}_{\text{RISR},i-1}\hat{\mathbf{x}}_{\text{RISR},i-1}^{H}\right)\odot\mathbf{I}_{N\times N} \tag{22}$$

for the ith iteration, where $\hat{\mathbf{x}}_{\text{RISR},i-1}$ is the previous estimate of the range profile. The adaptively estimated range profile at the ith iteration is therefore

$$\hat{\mathbf{x}}_{\text{RISR},i} = \mathbf{W}_{\text{RISR},i}^{H}\mathbf{y} = \hat{\mathbf{P}}_i\mathbf{W}^{H}\left(\mathbf{W}\hat{\mathbf{P}}_i\mathbf{W}^{H} + \sigma_u^2\mathbf{I}_{L\times L}\right)^{-1}\mathbf{y}, \tag{23}$$

which is initialized by the over-sampled matched filter estimate

$$\hat{\mathbf{x}}_{\text{RISR},0} = \hat{\mathbf{x}}_{\text{MF}} = \mathbf{W}^{H}\mathbf{y}. \tag{24}$$

V. Simulation Results

An LFM waveform with a bandwidth of 350MHz and pulse duration of 7μs is simulated and convolved with a scene containing multiple scatterers of disparate powers. The resulting signal is mixed with an LFM reference chirp having a bandwidth of 450MHz and a duration of 9μs. Both the LFM waveform and LFM reference have a chirp rate of 50 MHz/μs.

In the simulated scene shown in Fig. 2 there are 13 scatterers randomly distributed in range and with reflected powers that are randomly assigned from a uniform distribution on [−40 dB, 0 dB]. The matched filter bank result in blue is the result of standard stretch processing, where it is observed that the scatterers at 114 m and 154 m are obscured by the sidelobes of other nearby large scatterers. Clearly the optimal mismatch filter bank (green) and adaptive filter bank (red) yield significant improvement in terms of the visibility of scatterers that would otherwise be masked by sidelobes. Further, when the dynamic range is high we observe that adaptive filtering provides a sharper mainlobe response than the still rather good optimal mismatch filtering. The mismatch loss for both approaches is a small fraction of a dB.

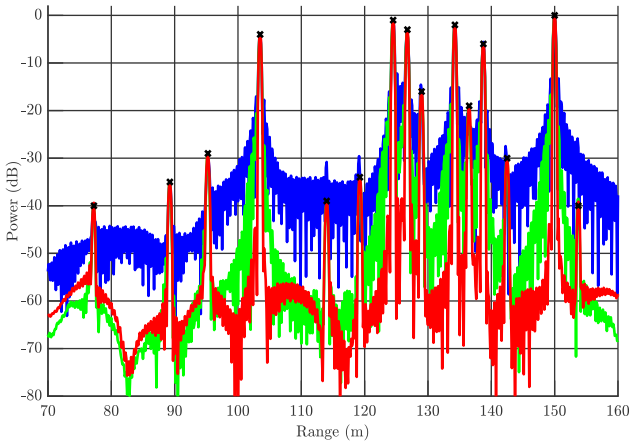

Fig. 2: Simulated range profile for standard stretch processing (blue), mismatch filtering (green), and adaptive filtering (red)

VI. Open-Air Experimental Results

Using the same LFM waveform and reference parameters from the previous section, open-air measurements were collected from the roof of Nichols Hall on the University of Kansas (KU) campus using the hardware instrumentation setup depicted in Fig. 3 that includes separate transmit and receive antennas and a stretch processing RF receive chain. The transmit center frequency was f_C = 3.5 GHz, such that the 350 MHz transmitted LFM waveform occupied a 10% bandwidth, and the transmit power was 24 dBm. For IQ sampling, a Rohde & Schwarz FSW 26 real-time spectrum analyzer (RSA) was used that has a sampling rate of f_S = 200 MHz with an analysis bandwidth of 160 MHz (from the lowpass filters in Fig. 1). A coherent processing interval (CPI) of 500 pulses was coherently averaged.

Fig. 3. Hardware instrumentation setup for open-air measurements

The illuminated scene of interest is the first 200 meters, for which the significant scatterers are annotated in Fig. 4. This region was selected because the direct path signal and nearby

scattering are captured with sufficient power in the receiver to provide as high a dynamic range as possible given the transmit power, so that the impact of optimal and adaptive mismatched filtering can be demonstrated.

Fig. 4: Annotated field of view for measured reults

Figure 5 compares the optimal mismatch filter response from (16) to the matched filter response (standard stretch processing) via (9) for measured data. It is observed that the optimal mismatched filter realizes roughly 10-15 dB of sidelobe suppression, particularly in the vicinity of the large direct path signal, and little mismatch loss (fraction of a dB). Figure 6 likewise compares the adaptive filtering response from (23) after 3 iterations of this stretch-RISR formulation, where 10-15 dB of sidelobe suppression and very low mismatch loss is likewise observed.

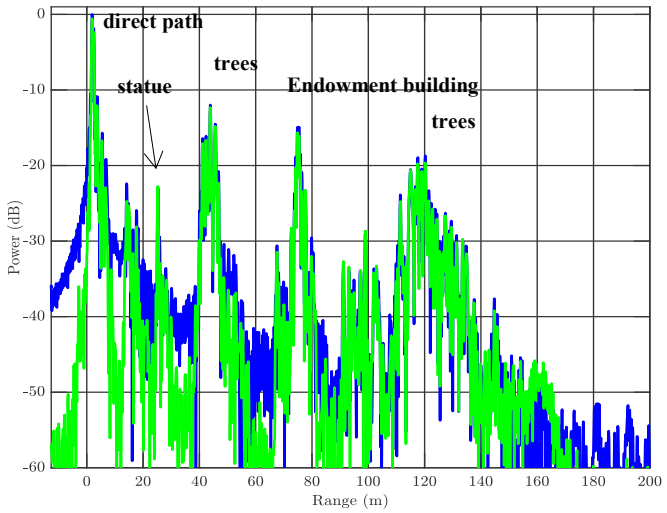

Fig. 5: Standard stretch processing (blue) and mismatch filter bank (green) for open-air measurements

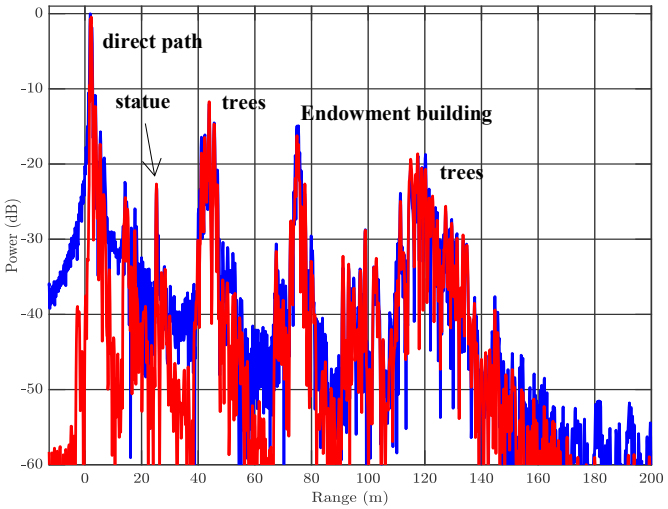

Fig. 6: Standard stretch processing (blue) and adaptive filter bank (red) for open-air measurements

Figure 7 shows all three methods for the first 50 meters so that finer detail can be discerned. For example, the optimal and adaptive mismatch filtering uncovers the small scatterer at a range of 8 meters that would otherwise have been masked by sidelobes for standard stretch processing. While one could potentially use some form of tapering to improve the sidelobe for standard stretch processing, such an approach also involves a trade-off in terms of SNR (due to tapering loss) and resolution degradation. For these new methods there is no resolution degradation and the mismatch loss is negligible.

These measured results show only rather minor differences between the optimal and adaptive mismatched filtering (e.g. narrower peak at 2 m and deeper nulls between some scatterers). However, the dynamic range of these measured results is at least 20 dB less than that of the simulated results in Fig. 2, and it is expected that further distinction could be observed if higher dynamic range were realized via higher transmit power.

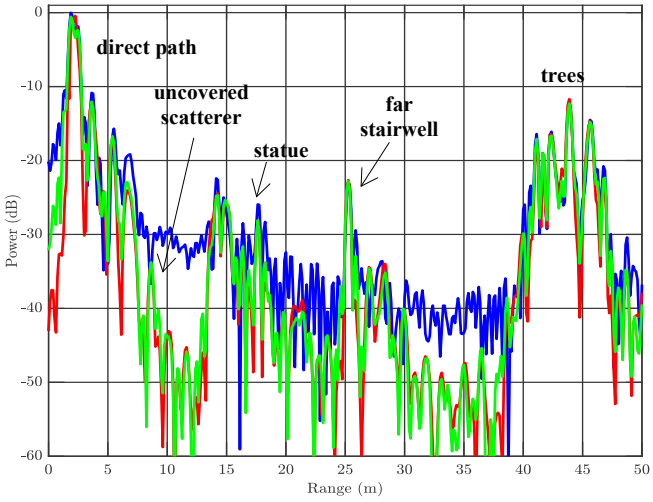

Fig. 7: Standard stretch processing (blue), mismatch filter bank (green), and adaptive filter bank (red) for first 50m of open-air measurements

VII. Conclusions

Stretch processing has been formulated using a linear model that permits the subsequent development of a least-squares based optimal mismatch filter bank and a mean-square error based adaptive filter bank. For high dynamic range scenarios these new methods provide significant sidelobe suppression enhancement without degrading range resolution and with negligible mismatch loss. In combination with the companion paper [4], these new filtering schemes can likewise be combined with other chirp-like nonlinear FM waveforms to provide greater design freedom for wideband radar applications that require high range resolution. In so doing, some of the new advantages promised by waveform diversity [21] can be applied to legacy radar systems that rely on stretch processing.

REF ERENCES

[1] W.J. Caputi, "Stretch: a time-transformation technique," *IEEE Trans. Aerospace & Electronic Systems*, vol. AES-7, no. 2, pp. 269-278, Mar. 1971.

[2] W.L. Melvin, J.A. Scheer, eds., *Principles of Modern Radar, Vol. II: Advanced Techniques*, SciTech Publishing, Edison, NJ, 2013, p. 26-40.

[3] J.R. Klauder, A.C. Price, S. Darlington, W.J. Albersheim, "The theory and design of chirp radars," *The Bell System Technical Journal*, vol. XXXIX, no. 4, pp. 745-808, July 1960.

[4] D.M. Hemmingsen, P.M. McCormick, S.D. Blunt, C. Allen, A. Martone, K. Sherbondy, D. Wikner, "Waveform-diverse stretch processing," submitted to *IEEE Radar Conf.*, Oklahoma City, OK, Apr. 2018.

[5] C.E. Cook, "A class of nonlinear FM pulse compression signals," *Proc. IEEE*, vol. 52, no. 11, pp. 1369-1371, Nov. 1964.

[6] E. Fowle, "The design of FM pulse compression signals," *IEEE Trans. Information Theory*, vol. 10, no. 1, pp. 61-67, Jan. 1964.

[7] I. Gladkova, "Design of frequency modulated waveforms via the Zak transform," *IEEE Trans. Aerospace & Electronic Systems*, vol. 40, no. 1, pp. 355-359, Jan. 2004.

[8] A.W. Doerry, "Generating nonlinear FM chirp waveforms for radar," *Sandia Report*, SAND2006-5856, Sept. 2006.

[9] S.D. Blunt, J. Jakabosky, M. Cook, J. Stiles, S. Seguin, and E.L. Mokole, "Polyphase-coded FM (PCFM) radar waveforms, part II: optimization," *IEEE Trans. Aerospace & Electronic Systems*, vol. 50, no. 3, pp. 2230-2241, July 2014.

[10] J. Jakabosky, S.D. Blunt, and B. Himed, "Optimization of 'over-coded' radar waveforms," *IEEE Radar Conf.*, Cincinnati, OH, May 2014.

[11] P.S. Tan, J. Jakabosky, J.M. Stiles, and S.D. Blunt, "On higher-order representations of polyphase-coded FM radar waveforms," *IEEE Intl. Radar Conf.*, Arlington, VA, May 2015.

[12] P.M. McCormick and S.D. Blunt, "Nonlinear conjugate gradient optimization of polyphase-coded FM radar waveforms," *IEEE Radar Conference*, Seattle, WA, May 2017.

[13] P.M. McCormick and S.D. Blunt, "Gradient-based coded-FM waveform design using Legendre polynomials," *IET International Conference on Radar Systems*, Belfast, UK, Oct. 2017.

[14] D. Henke, P. McCormick, S.D. Blunt, T. Higgins, "Practical aspects of optimal mismatch filtering and adaptive pulse compression for FM waveforms," *IEEE Intl. Radar Conf.*, Arlington, VA, May 2015.

[15] M.H. Ackroyd, F. Ghani, "Optimum mismatched filters for sidelobe suppression," *IEEE Trans. Aerospace & Electronic Systems*, vol. AES-9, no. 2, pp. 214-218, Mar. 1973.

[16] S.D. Blunt, K. Gerlach, "Adaptive pulse compression via MMSE estimation," *IEEE Trans. Aerospace & Electronic Systems*, vol. 42, no. 2, pp. 572-584, Apr. 2006.

[17] S.D. Blunt, T. Chan and K. Gerlach, "Robust DOA estimation: the reiterative superresolution (RISR) algorithm," *IEEE Trans. Aerospace & Electronic Systems*, vol. 47, no. 1, pp. 332-346, Jan. 2011.

[18] S.D. Blunt, M. Cook, J. Jakabosky, J. de Graaf, E. Perrins, "Polyphase-coded FM (PCFM) radar waveforms, part I: implementation," *IEEE Trans. Aerospace & Electronic Systems*, vol. 50, no. 3, pp. 2218-2229, July 2014.

[19] S.D. Blunt, K. Gerlach, T. Higgins, "Aspects of radar range super-resolution," *IEEE Radar Conf.*, Waltham, MA, Apr. 2007.

[20] W.L. Melvin, J.A. Scheer, *Principles of Modern Radar: Advanced Techniques*, SciTech Publishing, 2013, Chap 2.

[21] S.D. Blunt, E.L. Mokole, "An overview of radar waveform diversity," *IEEE AESS Systems Magazine*, vol. 31, no. 11, pp. 2-42, Nov. 2016.